The order of condensation in capillary grooves

FAST TRACK COMMUNICATION

The order of condensation in capillary grooves

Carlos Rascón[1], Andrew O Parry[1,2], Robert Nürnberg[2], Alessandro Pozzato[3,4], Massimo Tormen[3,4], Lorenzo Bruschi[5] and Giampaolo Mistura[5,6]

[1] GISC, Departamento de Matemáticas, Universidad Carlos III de Madrid, E-28911 Leganés, Madrid, Spain
[2] Department of Mathematics, Imperial College London, London SW7 2AZ, UK
[3] IOM-CNR, Laboratorio TASC, S.S. 14 Km 163.5, I-34149 Trieste, Italy
[4] ThunderNIL S.r.l., Via Ugo Foscolo 8, I-35131 Padova, Italy
[5] CNISM Unità di Padova, via Marzolo 8, I-35131 Padova, Italy
[6] Dipartimento di Fisica e Astronomia G.Galilei, Università di Padova, via Marzolo 8, I-35131 Padova, Italy

E-mail: carlos.rascon@uc3m.es

Abstract
We consider capillary condensation in a deep groove of width L. The transition occurs at a pressure $p_{co}(L)$ described, for large widths, by the Kelvin equation $p_{sat} - p_{co}(L) = 2\sigma \cos\theta/L$, where θ is the contact angle at the side walls and σ is the surface tension. The order of the transition is determined by the contact angle of the capped end θ_{cap}; it is continuous if the liquid completely wets the cap, and first-order otherwise. When the transition is first-order, corner menisci at the bottom of the capillary lead to a pronounced metastability, determined by a complementary Kelvin equation $\Delta p(L) = 2\sigma \sin\theta_{cap}/L$. On approaching the wetting temperature of the capillary cap, the corner menisci merge and a single meniscus unbinds from the bottom of the groove. Finite-size scaling shifts, crossover behaviour and critical singularities are determined at mean-field level and beyond. Numerical and experimental results showing the continuous nature of condensation for $\theta_{cap} = 0$ and the influence of corner menisci on adsorption isotherms are presented.

(Some figures may appear in colour only in the online journal)

The phase equilibria of confined fluids may be substantially different from that occurring in bulk [1]. Consider a simple fluid (or Ising magnet) between identical parallel walls, a distance L apart. In three dimensions (3D), the fluid exhibits coexistence between liquid and vapour-like phases but the first-order boundary and critical point are shifted (see figure 1). Below the bulk critical temperature T_c, vapour condenses at a pressure $p_{co}(L)$, less than that at saturation p_{sat}. For large L, the shift $\delta p_{co}(L) = p_{sat} - p_{co}(L)$ is described by the Kelvin equation [2–5]

$$\delta p_{co}(L) = \frac{2\sigma \cos\theta}{L} + \cdots \tag{1}$$

where σ is the surface tension and θ is the contact angle. This equation is usually derived by balancing free energies [4], but also has a simple geometrical interpretation; it identifies the radius $R = \sigma/\delta p$ of a circular meniscus that meets each wall at an angle θ [6]. Coexistence ends at a capillary critical point, where the distinction between the phases vanishes and the correlation length diverges. Finite-size scaling implies that the capillary critical temperature $T_c(L)$ satisfies [7, 8]

$$T_c - T_c(L) \propto L^{-1/\nu} \tag{2}$$

where $\nu \approx 0.63$ is the critical exponent of the 3D bulk correlation length. The amplitude of the shift depends weakly on the surface fields, implying that the wetting properties
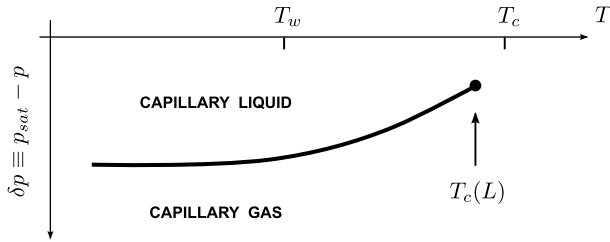
Figure 1. Schematic illustration of the location of first-order capillary condensation $\delta p_{co}(L)$ for a fluid between parallel walls. T_w is the wetting temperature of the substrate.
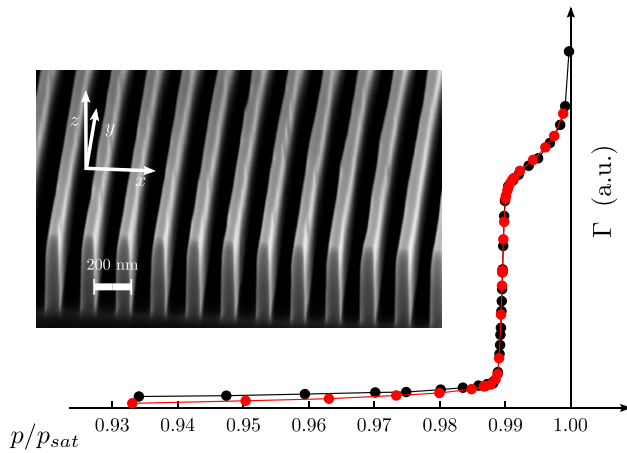
Figure 2. Overlaid adsorption (black) and desorption (red) isotherms ($T = 85$ K) for argon on the sculpted silicon substrate shown in the inset. The grooves have width $L \approx 90$ nm and depth $D \approx 500$ nm.

Figure 3. Total magnetization (in arbitrary units) versus bulk field h in a capillary of $L = 20$ and $D = 200$ (in units of the bulk correlation length) for different partial and complete wetting conditions at the side walls and cap. The numerical values of the bulk field at condensation (CO) and the spinodal (SP) are shown as vertical lines.

of the walls are not crucial. This is not the case if gas is preferentially adsorbed at one wall and liquid at the other, for which interfacial localization determines phase coexistence [9–12].

Modern techniques allow the fabrication of structured substrates in the laboratory, which has led to investigations of the influence of geometry on adsorption [6, 13–16]. For example, the inset of figure 2 shows an array of parallel grooves covering an area of about 1 cm^2 fabricated using nanoimprint lithography, wet etching and plasma etching in an inductively coupled plasma [17]. If the depth D is much larger than the width L, it is natural to expect that the adsorption is similar to that of the parallel plate geometry. However, recent theoretical studies reveal a surprising feature: for walls that are completely wet ($\theta = 0$) the condensation is continuous rather than first-order [18–22]. This change is due to the formation of a meniscus whose position moves from the cap to the open end as p is increased. An experimental verification of this is illustrated in figure 2, which shows the final portion of an adsorption isotherm taken with a torsional microbalance [23]. The attached sample is a thin silicon wafer with a side of about 1 cm and patterned with the rectangular wells shown in the inset. The vertical axis represents the moment of inertia of the adsorbed film as a function of the relative vapor pressure p/p_{sat} of argon at $T = 85$ K. The red symbols indicate the experimental adsorption isotherm (adding gas to the sample

cell), while the black symbols indicate the experimental desorption (removing gas). The capillary continuously fills with liquid at a pressure close to that predicted by the Kelvin equation with no hysteresis.

This leaves us with a number of questions: what happens if the contact angle θ is non-zero, or if the cap is made of a different material? The first point to recognize is that in a macroscopically deep groove there are two distinct transitions: condensation as $p \to p_{co}(L)^-$, and evaporation as $p \to p_{co}(L)^+$. Here, we use mean-field theory, effective Hamiltonian methods and scaling arguments to determine the order of these transitions, general critical behaviour and phase boundaries. We concentrate on systems with short-range forces and, for simplicity, choose walls that exhibit critical wetting. However, similar behaviour occurs for first-order wetting and long-range forces [23]. We have investigated the phase equilibria in a periodic array of grooves using a Landau theory similar to that used for the parallel plate geometry [7, 8, 10]. We use a magnetic notation, and determine the magnetization $m(z, x)$ by minimizing

$$F[m] = \iint dx\,dz\left(\tfrac{1}{2}(\nabla m)^2 + \Phi(m) - mh\right) + F_s \quad (3)$$

where $\Phi(m) = (m^2 - t)^2/8$, $t \propto T_c - T$, and h is the bulk field (analogous to $p - p_{sat}$). Thus, the bulk magnetization is $m_0(T) = \pm\sqrt{t}$ for $T < T_c$. The surface integral along the walls is $F_s = \int ds(cm^2/2 - h_s m)$, where the surface enhancement c is larger than the inverse bulk correlation length, ensuring critical wetting boundary conditions, and the surface field is $h_s = h_1$ except at the cap ($h_s = h_{cap}$). These two values of h_s lead to distinct contact angles: θ at the side walls and θ_{cap} at the cap. In particular, the wetting temperatures for the side and capped walls are determined by $cm_0(T_w) = h_1$ and $cm_0(T_w^{cap}) = h_c$, respectively [24]. Far above the capillary opening, the magnetization is fixed to $-m_0$, modelling a bulk vapour.

a)

b)

c)
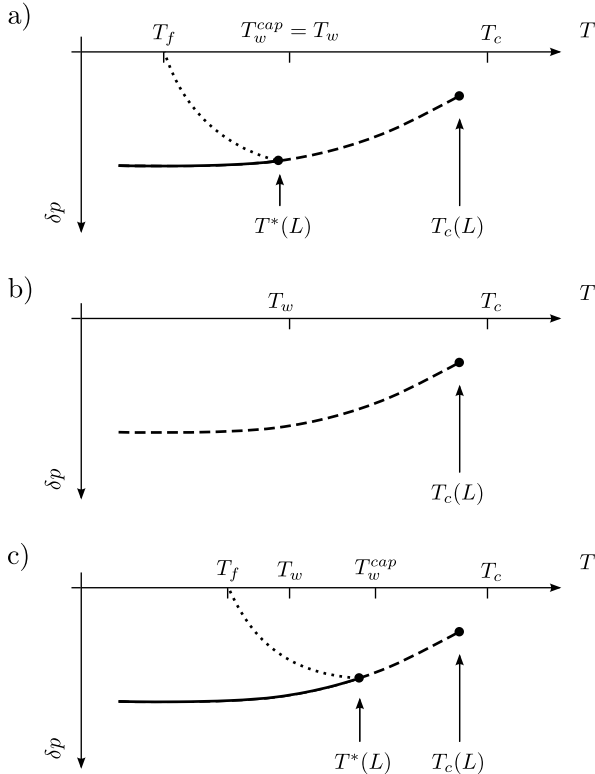
Figure 4. Schematic condensation phase diagrams for capillaries with the same walls as in figure 1 but different caps: (a) the cap is the same material as the walls, (b) the liquid completely wets the cap and (c) the liquid wets the cap at a higher temperature than the side walls. Solid, dashed and dotted lines represent first-order condensation, continuous condensation and spinodal lines, respectively.

Our results are as follows.

(1) The order of the capillary condensation is determined by the wetting properties of the capped end. Macroscopically, the transition is first-order if the liquid partially wets the cap, while it is continuous if $\theta_{\mathrm{cap}} = 0$. The wetting properties of the sides only determine $\delta p_{\mathrm{co}}(L)$, as for the parallel plate geometry. This is illustrated by the different adsorption isotherms in figure 3. The corresponding condensation phase diagrams are shown in figure 4, where the dashed and solid lines lie on the condensation curve for the parallel plate geometry of figure 1. The dashed lines represent continuous condensation, and extend from $T_{\mathrm{c}}(L)$ to $T^*(L) \approx T_{\mathrm{w}}^{\mathrm{cap}}$, while the solid lines below $T^*(L)$ represent first-order coexistence. Examples of coexisting phases are shown in figure 5 and show separate menisci forming at the corners.

(2) The gas phase has a metastable extension ending in a spinodal line $p_{\mathrm{s}}(L)$ (figure 4). This instability has a geometrical interpretation similar to that of the Kelvin equation, and occurs when the circular menisci coalesce in the middle of the groove (see figure 5(c)). Provided $p_{\mathrm{s}}(L) < p_{\mathrm{sat}}$, the width of the metastable region, $\Delta p(L) = p_{\mathrm{s}}(L) - p_{\mathrm{co}}(L)$, is

$$\Delta p(L) = \frac{2\sigma \sin\theta_{\mathrm{cap}}}{L} + \cdots \qquad (4)$$

and accurately describes the numerically determined spinodal for L larger than about 20 bulk correlation lengths. Note that

COEXISTING STATES   SPINODAL STATES
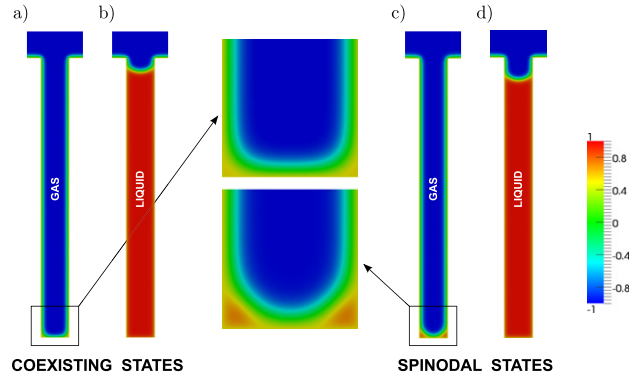
Figure 5. Numerically determined magnetization profiles for a capillary with $\theta = \theta_{\mathrm{cap}} = 46.6°$, $L = 20$ and $D = 200$ (in units of the bulk correlation length). Here, (a) and (b) are the coexisting vapour-like and liquid-like phases at $p = p_{\mathrm{co}}(L)$, while (c) and (d) correspond to the gas and liquid spinodals, respectively.

$\Delta p(L)$ vanishes as $T \to T_{\mathrm{w}}^{\mathrm{cap}}$, signalling that the condensation becomes second-order. When the walls and cap are the same, capillary condensation is continuous above T_{w} and first-order below it. However, if $T_{\mathrm{w}}^{\mathrm{cap}} < T_{\mathrm{w}}$, the first-order line is reduced, and is eventually suppressed when $\theta_{\mathrm{cap}} = 0$. On the other hand, if $T_{\mathrm{w}}^{\mathrm{cap}} > T_{\mathrm{w}}$, the continuous condensation line is reduced and is suppressed when $\theta_{\mathrm{cap}} \geq \pi/2$, recovering the condensation phase diagram of the parallel plate geometry. Equation (4) is only valid for $T > T_{\mathrm{f}}$, where T_{f} is the corner filling temperature at which $\theta_{\mathrm{cap}} + \theta = \pi/2$ [25–29]. For $T < T_{\mathrm{f}}$, the adsorption at the corners is microscopic [23].

(3) On approaching $T^*(L)$ along $p_{\mathrm{co}}(L)$, the corner menisci merge to form a single stable meniscus, the height of which, ℓ_{m}, diverges continuously. Thus, $T^*(L)$ acts as a wetting temperature for the unbinding of the meniscus [30]. At mean-field level, the shift of $T^*(L)$ from $T_{\mathrm{w}}^{\mathrm{cap}}$ is exponentially small in the slit width, and $\ell_{\mathrm{m}} \approx -\xi_{\mathrm{l}}(L) \ln(T^*(L) - T)$. Here, $\xi_{\mathrm{l}}(L)$ is the correlation length of the capillary liquid phase, although, away from the vicinity of $T_{\mathrm{c}}(L)$, this is indistinguishable from the correlation length of the bulk liquid ξ_{l}. However, these mean-field predictions are incorrect, due to crossover from 3D to 2D unbinding. This can be understood using an interfacial model $H[\ell] = \int \mathrm{d}y(\frac{\sigma_{\mathrm{eff}}}{2}(\mathrm{d}\ell/\mathrm{d}y)^2 + W_{\mathrm{cap}}(\ell))$, where $\ell(y)$ is the height of the meniscus along the groove. The bending of the meniscus along the groove is resisted by an effective stiffness $\sigma_{\mathrm{eff}} \approx \sigma L$, while the binding to the cap is modelled by an attractive potential W_{cap} of depth $\sigma L \theta_{\mathrm{cap}}^2$ and range $L\theta_{\mathrm{cap}}$. Solution of this model shows that the meniscus unbinds when $L\theta_{\mathrm{cap}}^* \approx \sqrt{k_{\mathrm{B}}T/\sigma}$. This is equivalent to

$$T_{\mathrm{w}}^{\mathrm{cap}} - T^*(L) \propto (\omega^{-\frac{1}{2}}L)^{-1/\nu_{\parallel}} + \cdots \qquad (5)$$

where $\omega = k_{\mathrm{B}}T/4\pi\sigma\xi_{\mathrm{l}}^2$ and $\nu_{\parallel}$ is the exponent of the parallel correlation length for 3D short-range critical wetting, $\xi_{\parallel} \approx (T_{\mathrm{w}}^{\mathrm{cap}} - T)^{-\nu_{\parallel}}$. In Ising model simulations [31], the observed value of this exponent is $\nu_{\parallel} \approx 1.3$, which is slightly larger than the mean-field prediction but much smaller than the non-universal, ω dependent, value predicted by simple interfacial models [30]. This is likely due to non-local interfacial interactions [32, 33]. The wetting temperature
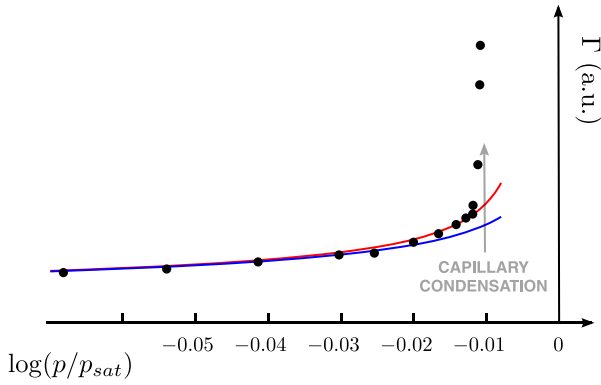
Figure 6. Detail of the experimental adsorption isotherm of figure 1 close to continuous condensation. The solid lines show the theoretical prediction for the adsorption arising from the wetting films alone (lower curve) and including the additional contribution from the corner menisci (upper curve).

shift (5) may be an alternative route to measuring $\nu_\parallel$ in Ising model simulation studies. As $T \to T^*(L)$, the meniscus height changes from the 3D-like logarithmic growth to $\ell_m \propto (\sigma L (T^*(L) - T))^{-1}$ although, for wide slits, the asymptotic regime will be small. The scaling law (5) refers to the limit $L \to \infty$. However, $T^*(L)$ tends to $T_c(L)$ for fixed L, as $\theta \to \pi/2$. This can be understood from surface scaling theory [7, 34]; we find $T_c(L) - T^*(L) \propto L^\phi h_{cap}^2$ as $h_{cap} \to 0$. Here, $\phi = (2\Delta_1 - 1)/\nu$, where $\Delta_1 \approx 0.45$ is the 3D surface gap exponent, implying $\phi \approx -0.16$. The power-law dependence on L means that $T^*(L)$ is determined by T_w^{cap} for all but the weakest fields h_{cap}.

(4) The continuous condensation occurring for $T_c(L) > T > T^*(L)$ exhibits different regimes, showing the influence of geometry, intermolecular forces and fluctuation effects as $p \to p_{co}(L)$. At a macroscopic level, the adsorption arises from the two corner menisci, which merge exactly at $p = p_{co}(L)$ and precipitate the filling of the capillary. The easiest way of incorporating interactions is to combine this with the adsorption from the microscopic wetting films which coat the substrate [6]. Indeed, away from the immediate vicinity of the condensation transition, this accurately reproduces the experimental adsorption isotherms (see figure 6). In a very narrow regime sufficiently close to $p_{co}(L)$, the menisci merge forming a single meniscus. This occurs when the menisci are at a distance $\xi_\parallel$ apart, corresponding to the parallel correlation length for the wetting layer of the cap. At mean-field level, this occurs for $p_{co}(L) - p \ll \sqrt{\sigma^2 \xi_1 / L^3}$, and the height ℓ_m of the single meniscus diverges as

$$\ell_m \approx -\xi_1 \ln(p_{co}(L)/p - 1) \tag{6}$$

where the logarithmic growth is characteristic of short-range 3D complete wetting transition. Beyond mean-field and even closer to condensation $(p_{co}(L) - p \ll (k_B T)^2 / \sigma L^2)$, fluctuations in the height of the meniscus along the groove lead to crossover to 2D-like complete wetting and alter this to $\ell_m \propto L^{-2/3} |p_{co}(L) - p|^{-1/3}$ [20]. The line of continuous condensation ends at $T_c(L)$, where the meniscus disappears, and there is critical adsorption from the long-range decay of the profile away from the cap.

(5) In a macroscopically deep groove, the evaporation transition is continuous for all T and independent of the cap properties. However, the divergence of the meniscus depth $\widetilde{\ell}_m = D - \ell_m$ from the top of the groove is very different above and below the wetting temperature T_w. Mean-field calculations show that the meniscus unbinds as $\widetilde{\ell}_m \approx -\xi_g(L) \ln(p/p_{co}(L) - 1)$, where the coefficient $\xi_g(L)$ is the correlation length of the confined gas phase. Far below the wetting temperature of the side walls, $\xi_g(L)$ is similar to the correlation length of the bulk gas. However, above the wetting temperature, $\xi_g(L)$ is determined by the parallel correlation length of the complete wetting layers [35], so that $\xi_g(L) \approx \sqrt{\sigma \xi_1 / \delta p}$. On making use of the Kelvin equation, it follows that

$$\widetilde{\ell}_m \approx -\sqrt{\frac{\xi_1 L}{2}} \ln(p/p_{co}(L) - 1) \tag{7}$$

compared with (6) for the condensation side. Therefore, for $\theta = \theta_{cap} = 0$, the adsorption isotherms will be strongly asymmetric about $p_{co}(L)$.

We mention that similar phenomena occur in grooves of finite depth D. When $D \gg L$ the transition order is again determined by the wetting properties of the capped end. Above a certain temperature $T^*(L, D) \lesssim T^*(L)$, the capillary fills abruptly but continuously as p is increased through $p_{co}(L)$ (figure 3(a)). Below this temperature, there is coexistence for $p \approx p_{co}(L)$ between two distinct phases in which the meniscus is either pinned near the groove bottom or near the top. The coexisting states become indistinguishable at $T^*(L, D)$, which represents a critical point (belonging to the 2D Ising universality class) rather than the meniscus unbinding transition occurring for the infinitely deep groove. The phase equilibrium is therefore very similar to that occuring for fluids between competing walls [9–12], where the meniscus plays the role of the delocalizing interface, but occurring in one dimension lower. When the grooves are no longer deep, $D \approx L$, one may lose first-order condensation entirely, similarly to studies of wetting on corrugated and striped walls [36–38].

Finally, if we consider a single groove instead of an array, similar phenomena occur although, of course, phase coexistence and criticality are rounded beyond mean-field because the geometry is pseudo-one-dimensional. Thus, for $T \lesssim T^*(L, D)$, domains will form along the groove in which the meniscus is pinned to the bottom or top. However, the characteristic size of these domains scales as $e^{\sigma L D / k_B T}$, so that the rounding of the first-order condensation will be unobservable.

In summary, we have shown that the condensation of vapour in a capillary groove is controlled by the wetting properties of the cap. The location of the transition is given by the Kelvin equation, but its order is determined by a complementary result, due to the behaviour of corner menisci. We anticipate that the shape or roughness of the cap is also important, and that this may allow the further tuning of the transition order.

References

[1] Evans R 1990 *J. Phys.: Condens. Matter* **2** 8989
Gelb L D, Gubbins K E, Radhakrishnan R and Sliwinska-Bartkowiak M 1999 *Rep. Prog. Phys.* **62** 1573
Saam W F 2009 *J. Low Temp. Phys.* **157** 77 and references therein

[2] Thomson W 1871 *Phil. Mag.* series 4 **42** 448

[3] Derjaguin B V 1940 *Zh. Fiz. Khim.* **14** 137

[4] Evans R, Marini Bettolo Marconi U and Tarazona P 1986 *J. Chem. Phys.* **84** 2376

[5] Parry A O and Evans R 1992 *J. Phys. A: Math. Gen.* **25** 275

[6] Rascón C and Parry A O 2000 *Nature* **407** 986

[7] Fisher M E and Nakanishi H 1981 *J. Chem. Phys.* **75** 5857

[8] Nakanishi H and Fisher M E 1983 *J. Chem. Phys.* **78** 3279

[9] Albano E V, Binder K, Heermann D W and Paul W 1989 *Surf. Sci.* **223** 151

[10] Parry A O and Evans R 1990 *Phys. Rev. Lett.* **64** 439

[11] Swift M R, Owczarek A L and Indekeu J O 1991 *Europhys. Lett.* **14** 475

[12] Albano E V and Binder K 2009 *J. Stat. Phys.* **135** 991

[13] Bruschi L, Carlin A and Mistura G 2002 *Phys. Rev. Lett.* **89** 166101

[14] Gang O, Alvine K J, Fukuto M, Pershan P S, Black C T and Ocko B M 2005 *Phys. Rev. Lett.* **95** 217801

[15] Tasinkevych M and Dietrich S 2006 *Phys. Rev. Lett.* **97** 106102

[16] Hofmann T, Tasinkevych M, Checco A, Dobisz E, Dietrich S and Ocko B M 2010 *Phys. Rev. Lett.* **104** 106102

[17] Pozzato A, Dal Zilio S, Bruschi L, Mistura G and Tormen M 2009 *Microelectron. Eng.* **86** 1329

[18] Marconi U M B and Van Swol F 1989 *Phys. Rev.* A **39** 4109–16

[19] Darbellay G A and Yeomans J M 1992 *J. Phys. A: Math. Gen.* **25** 4275–83

[20] Parry A O, Rascón C, Wilding N B and Evans R 2007 *Phys. Rev. Lett.* **98** 226101

[21] Roth R and Parry A O 2011 *Mol. Phys.* **109** 1159

[22] Malijevsky A 2012 *J. Chem. Phys.* **137** 214704

[23] Bruschi L, Carlin A, Parry A O and Mistura G 2003 *Phys. Rev.* E **68** 021606

[24] Nakanishi H and Fisher M E 1982 *Phys. Rev. Lett.* **49** 1565

[25] Rejmer K, Dietrich S and Napiórkowski M 1999 *Phys. Rev.* E **60** 4027

[26] Parry A O, Rascón C and Wood A J 1999 *Phys. Rev. Lett.* **83** 5535

[27] Parry A O, Rascón C and Wood A J 2000 *Phys. Rev. Lett.* **85** 345

[28] Jakubczyk P and Napiorkowski M 2002 *Phys. Rev.* E 041107

[29] Milchev A, Müller M, Binder K and Landau D P 2003 *Phys. Rev. Lett.* **90** 136101

[30] For reviews of wetting, see Dietrich S 1988 *Phase Transitions and Critical Phenomena* vol 12, ed C Domb and J L Lebowitz (New York: Academic)
Schick M 1990 *Liquids at Interfaces* ed J Charvolin, J F Joanny and J Zinn-Justin (Amsterdam: Elsevier) p 3364
Bonn D *et al* 2009 *Rev. Mod. Phys.* **81** 739

[31] Albano E V and Binder K 2012 *Phys. Rev. Lett.* **109** 036101

[32] Parry A O, Romero-Enrique J M and Lazarides A 2004 *Phys. Rev. Lett.* **93** 086104

[33] Parry A O, Rascón C, Bernardino N and Romero-Enrique J M 2008 *Phys. Rev. Lett.* **100** 136105

[34] Binder K, Landau D P and Wansleben S 1989 *Phys. Rev.* B **40** 6971

[35] Parry A O, Bernardino N R and Rascón C 2011 *Mol. Phys.* **109** 1015

[36] Rascón C, Parry A O and Sartori A 1999 *Phys. Rev.* E **59** 5697

[37] Bauer C and Dietrich S 1999 *Eur. Phys. J.* B **10** 767

[38] Rascón C and Parry A O 2001 *J. Chem. Phys.* **115** 5258